



CrossMark
click for updates

Cite this: DOI: 10.1039/c5cy01433f

Copper supported on H⁺-modified manganese oxide octahedral molecular sieves (Cu/H-OMS-2) as a heterogeneous biomimetic catalyst for the synthesis of imidazo[1,2-a]-N-heterocycles†

Xu Meng,^a Jinqi Zhang,^a Baohua Chen,^b Zhenqiang Jing^c and Peiqing Zhao^{*a}

Copper supported on acid-modified manganese oxide octahedral molecular sieves (Cu/H-OMS-2) was prepared and found to be a versatile catalyst for the oxidative synthesis of 3-arylimidazopyridines with a broad substrate scope. Cu/H-OMS-2 that was characterized by BET, XRD, XPS, FTIR, TEM, SEM, H₂-TPR and O₂-TPD techniques could also be used to synthesize 3-arylimidazopyrimidines and applied in one-pot, three-component reactions of ketones, aldehydes and 2-aminopyridines. The catalytic system employs low loading Cu as the catalytic metal and support H-OMS-2 as the electron-transfer mediator (ETM) to sequentially lower the redox energy barrier, which generates a low-energy pathway and enables the reaction to proceed in a biomimetic way. Moreover, Cu/H-OMS-2 could be reutilized 4 times with a slight decrease in the catalytic activity.

Received 28th August 2015,
Accepted 21st October 2015

DOI: 10.1039/c5cy01433f

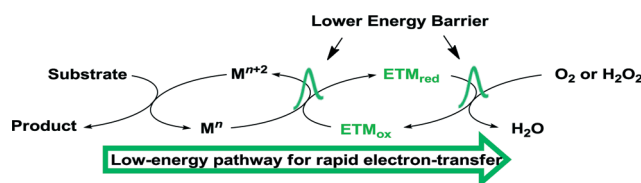
www.rsc.org/catalysis

Introduction

Within the past decades, OMS-2, microporous tunnel-structured manganese oxide octahedral molecular sieves, has attracted great interest in catalysis as well as materials and environmental science.¹ In particular, OMS-2 has been treated as a versatile redox catalyst in various oxidations because it has superior properties, such as excellent structural stability, mixed valence, large surface areas, electron-conducting properties and oxygen reduction abilities.^{2,3} Meanwhile, modified OMS-2 *via* ion exchange has also been prepared and applied in oxidations.⁴ Moreover, OMS-2 has been employed as a support of the supported catalysts in heterogeneous catalysis, which was fruitfully used in CO oxidation,⁵ VOC combustion⁶ and the removal of HCBz.⁷ Therefore, developing useful and sustainable catalytic systems by the use of OMS-2 is desirable and challenging.

From the perspective of redox potential, mixed valent OMS-2 that works as a support and an electron-transfer

mediator (ETM)⁸ at the same time can interact with the supported catalytic metal (M) to lower the energy barrier of an oxidation in theory as long as the redox potential of OMS-2 is between the potential of M_{red}/M_{ox} and green oxidant O₂/H₂O (Scheme 1).⁹ In this way, electrons of an oxidative transformation can rapidly transfer from the substrate to the oxidant in a biomimetic way by the use of ETM, which enhances the catalytic efficiency, lowers the catalytic metal loading, enables O₂ to be an efficient oxidant and produces water as the sole by-product. On the basis of this strategy, we previously developed the heterogeneous biomimetic CuO_x/OMS-2-catalyzed synthesis of 3-iodoimidazopyridines using air as the oxidant under a low-energy pathway.^{9a} Likewise, Mizuno's group previously reported a biomimetic homocoupling of alkynes catalyzed by Cu(OH)_x/OMS-2.^{9b} Our continued interest in this field prompts us to discover other efficient and novel OMS-2-based catalytic systems that are able to sequentially decrease the redox energy barriers in oxidative transformations.



Scheme 1 The oxidations involve the use of ETM under a long-energy pathway.

^a State Key Laboratory for Oxo Synthesis and Selective Oxidation, Suzhou Research Institute of LICP, Lanzhou Institute of Chemical Physics (LICP), Chinese Academy of Sciences, Lanzhou 730000, China. E-mail: zhaopq@licp.cas.cn; Fax: + 96 931 8277008; Tel: + 86 931 4968688

^b State Key Laboratory of Applied Organic Chemistry, Lanzhou University, Lanzhou, 730000, China

^c Suzhou Institute of Nano-Tech and Nano-Bionic (SINANO), Chinese Academy of Sciences, Suzhou 215123, China

† Electronic supplementary information (ESI) available. See DOI: 10.1039/c5cy01433f

Imidazo[1,2-*a*]pyridines are very important structural motifs and have been found in various biologically active and pharmaceutical compounds because they are antiviral, antimicrobial, antitumour, anti-inflammatory, antiparasitic, hypnotic, *etc.*¹⁰ Many commercial drugs involve imidazopyridines, like zolpidem, zolimidine, alpidem, saripidem and necopidem.¹¹ Especially, 3-arylimidazo[1,2-*a*]pyridines exhibit excellent anticancer properties.¹² The most traditional method of obtaining 3-arylimidazo[1,2-*a*]pyridines is functionalization of imidazo[1,2-*a*]pyridines in three steps, including formylation, Grignard reaction and oxidation.^{12a} Most recently, homogeneous Cu-catalyzed oxidative cyclizations for the synthesis of 3-arylimidazo[1,2-*a*]pyridines from chalcones and 2-aminopyridines *via* C–N bond forming were developed.¹³ Nevertheless, the aforementioned homogeneous catalysis generally produces a small amount of by-products, like Michael adducts and another cyclized product, naphthyridines,¹⁴ because of the high level of activity derived from its uniformity on a molecular level and solubility in the reaction medium. In addition, the separation, recovery and recycling of catalysts are relatively hard to achieve in homogeneous reactions.¹⁵ So, there is an incentive to develop a heterogeneous process able to produce 3-arylimidazo[1,2-*a*]pyridines by an environmentally friendly concept while minimizing the by-products and wastes.

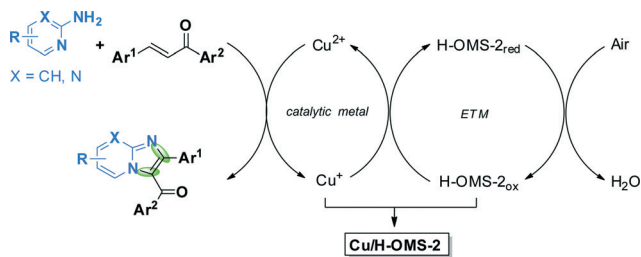
As a part of our continuing efforts on developing efficient heterogeneous catalytic systems and their applications in organic transformations,^{3e,9a} we now present the study of immobilized copper on H⁺-modified OMS-2 as a catalyst (Cu/H-OMS-2) that can sequentially decrease the energy barrier of the oxidation and generate a low-energy pathway in the synthesis of 3-arylimidazo[1,2-*a*]pyridines in air (Scheme 2). The heterogeneous system can also tolerate 2-aminopyrimidine as a substrate and offer 3-arylimidazo[1,2-*a*]pyrimidines in good yields. Furthermore, the desired heterocycles can be obtained *via* one-pot, three-component reactions of aldehydes, ketones and aminopyridines using Cu/H-OMS-2.

Results and discussion

Cu/H-OMS-2 was prepared *via* wet impregnation using Cu(NO₃)₂·3H₂O as the copper precursor in deionized water. Elemental analysis of the catalyst by atomic absorption

spectrometry (AAS) showed that the quantities of Cu in the sample was 1.58 wt%. The BET surface areas and porosities of Cu/H-OMS-2 were determined by N₂ adsorption-desorption at 77 K, and the results showed that the BET surface area is 87 m² g^{−1}, the pore volume is 0.4 cm³ g^{−1} and the pore size is 136 Å. X-ray diffraction (XRD) was employed to characterize OMS-2, H-OMS-2 and Cu/H-OMS-2 (Fig. 1, left). XRD patterns showed that the diffraction peaks of H-OMS-2 and Cu/H-OMS-2 were the same as that of OMS-2, which means both Cu/H-OMS-2 and its support are typical cryptomelane materials (JCPDS file #29-1020). No signals due to copper metal (cluster) or copper oxide were observed, which indicates that the copper oxide was low loading and highly dispersed on H-OMS-2. Notably, the diffraction peaks of Cu/H-OMS-2 and H-OMS-2 became slightly narrower and sharper compared with OMS-2, which suggests that their crystallite sizes increased. The lattice vibrational behaviour of the Cu/H-OMS-2 was studied by FTIR spectroscopy to detect the effect of Cu and H⁺ substitution on the spectral features of OMS-2. As shown in Fig. 1 (right), we obtained similar IR spectra from OMS-2, H-OMS-2 and Cu/H-OMS-2. All samples displayed four characteristic bonds at 714 cm^{−1}, 606 cm^{−1}, 521 cm^{−1} and 465 cm^{−1} with comparable relative intensities that can be ascribed to Mn–O lattice vibration modes in MnO₆ octahedra.¹⁶ Additionally, TEM images showed that H-OMS-2 and Cu/H-OMS-2 (for the SEM image, see the ESI† Fig. S1) have a typical nano-rod morphology,⁴ which means the acid modification and the supported copper do not change the structure of OMS-2 (Fig. 2).

The redox ability of Cu/H-OMS-2 was measured by means of H₂-TPR, while support H-OMS-2 and OMS-2 were also examined for comparison. For all OMS-2-based materials, the reduction of MnO₂ to MnO proceeds in two different steps (MnO₂ to Mn₃O₄ to MnO) generally, but these processes overlap sometimes.^{5a} As shown in Fig. 3, the overlapping peaks (a) from 369 °C to 395 °C are ascribed to the reduction of MnO₂ to MnO of OMS-2. For H-OMS-2, the two reduction peaks (b and b') of MnO₂ which were demonstrated at 345 °C and 387 °C shifted to lower temperatures, suggesting that the reducibility of H-OMS-2 was improved by H⁺ modification. Furthermore, two new peaks (α and β) appeared at temperatures in the range of 250–300 °C, which are ascribed to the partial reduction of MnO₂ species derived from the interaction between H⁺ and MnO₂.^{5a} Specifically, the α peak



Scheme 2 Cu-catalyzed multistep oxidation using H-OMS-2 as an ETM for the synthesis of imidazo[1,2-*a*]pyridines and imidazo[1,2-*a*]pyrimidines.

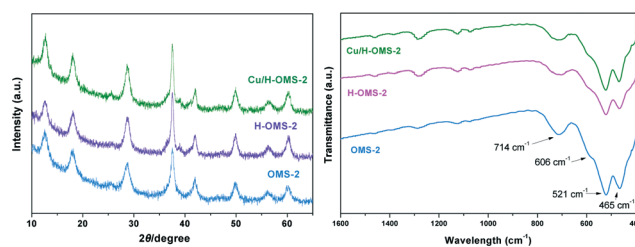


Fig. 1 XRD (left) and IR spectra (right) of OMS-2, H-OMS-2 and Cu/H-OMS-2.

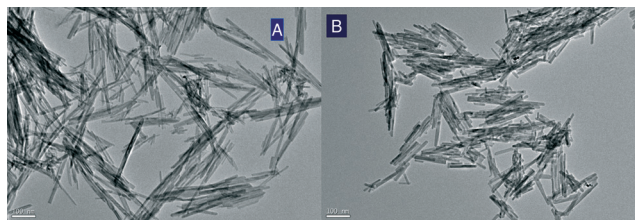


Fig. 2 TEM images of H-OMS-2 (A) and CuO/H-OMS-2 (B).

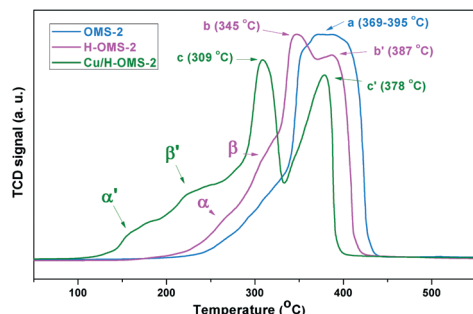


Fig. 3 H_2 -TPR of OMS-2, H-OMS-2 and Cu/H-OMS-2.

probably corresponds to the reduction of $MnO_6-\square$ (where \square stands for oxygen vacancies) and the β peak likely corresponds to the reduction of MnO_6-K^+ and MnO_6-H^+ . For Cu/H-OMS-2, four reduction peaks (c, c', α' and β') all shifted to lower temperatures compared with support H-OMS-2 and OMS-2, implying further enhanced redox ability. In particular, the α' peak generally corresponds not only to the reduction of well-dispersed CuO particles but also to the partial reduction of MnO_2 species. The improved reduction of MnO_2 is due to the spillover hydrogen from copper atoms to manganese oxides. It is believed that β' peak corresponds to the combined reduction of large CuO particles and MnO_2 .^{5a} Cu/H-OMS-2 has larger α' and β' peaks and more obvious c and c' peaks, which probably indicates that $Cu^{2+}-O-Mn^{4+}$ entities were formed at the interface between CuO and H-OMS-2 and the mobility of oxygen was promoted by the electronic delocalization effect between Cu and Mn species.^{5b,7} Furthermore, the XPS of Mn 2p from H-OMS-2 and Cu/H-OMS-2 also indicates that there is an interaction between copper and H-OMS-2 (for detailed discussion, see the ESI† Fig. S2). The phenomenon of electron transfer between the catalytic metal copper and the electron-transfer mediator H-OMS-2 probably can be proved from these observations.

Then, O_2 -TPD technology was used to analyze the oxygen species of Cu/H-OMS-2. As shown in Fig. S3 (see the ESI†), very similar peaks from the desorption of H-OMS-2 and Cu/H-OMS-2 were obtained, and the majority of oxygen species can be ascribed to lattice oxygen.⁷ Specifically, the similar and clear shoulder peaks at around 500 °C can be ascribed to surface oxygen species or the labile oxygen species. The peaks at around 600 °C and 750 °C result from the transformation of cryptomelane to Mn_2O_3 and further to Mn_3O_4 .¹⁷ Oxygen atoms in the framework bound to Mn(III) have a weaker

interaction compared with the interaction between oxygen atoms and Mn(IV), so two different oxygen species were released at middle temperature and high temperature, respectively, during TPD.

The oxidative cyclization between 2-aminopyridine and chalcone was selected as a model reaction to test the catalytic activity of Cu/H-OMS-2 (Table 1). From a synthetic point of view, the copper-catalyzed cyclization of 1a and 2a will lead to 3-arylimidazo[1,2-a]pyridine as the desired product with 3aa and another product, naphthyridine, which comes from a competitive cyclization, as by-products.¹⁴ Michael adduct 3aa actually is the intermediate during the formation of 3a, which means the high yield of 3a depends on the efficient formation of 3aa firstly and its subsequent intermolecular oxidative cyclization. So, we screened different parameters, such as the catalyst, the solvent and the temperature, to determine the best catalytic system for obtaining high yield of 3-arylimidazo[1,2-a]pyridine. In the initial experiment, OMS-2 was treated with reactants in DCB at 80 °C in air for 20 h, which did not show any catalytic activity (Table 1, entry 1). When we switched the catalyst to Cu/OMS-2 under the same conditions, 3a and 3aa were both obtained in low yields (Table 1, entry 2). However, the formation of 3a failed to proceed using $Cu(OH)_x/OMS-2$ as a catalyst (Table 1, entry 3). An attempt to employ Cu/H-OMS-2 (12 mg, 0.7 mol%, Cu: 1.58 wt%) in the synthesis of 3-arylimidazo[1,2-a]pyridine

Table 1 Optimization of reaction conditions^a


				Yield ^b (%)	
Entry	Catalyst	Solvent	T [°C]	3a	3aa
1	OMS-2	DCB	80	0	0
2 ^c	Cu/OMS-2	DCB	80	15	28
3 ^d	$Cu(OH)_x/OMS-2$	DCB	80	0	<5
4	Cu/H-OMS-2	DCB	80	10	18
5	Cu/H-OMS-2	DCB	100	23	<5
6	Cu/H-OMS-2	DMSO	100	8	12
7	Cu/H-OMS-2	MeNO ₂	100	8	<5
8	Cu/H-OMS-2	Toluene	100	13	25
9 ^e	Cu/H-OMS-2	HOAc	100	0	59
10	Cu/H-OMS-2	$Cl_2CHCHCl_2$	100	41	0
11 ^f	Cu/H-OMS-2	$Cl_2CHCHCl_2/HOAc$	100	89	0
12 ^f	Cu/H-OMS-2	Xylene/HOAc	100	12	0
13 ^f	Cu/H-OMS-2	Dioxane/HOAc	100	10	0
14 ^f	Cu/H-OMS-2	DMF/HOAc	100	<5	0
15 ^{f,g}	Cu/H-OMS-2	$Cl_2CHCHCl_2/HOAc$	100	42	16
16 ^f	Cu/H-OMS-2	$Cl_2CHCHCl_2/HOAc$	70	0	0
17 ^f	Cu/H-OMS-2	$Cl_2CHCHCl_2/HOAc$	120	76	0
18 ^{f,h}	CuO + H-OMS-2	$Cl_2CHCHCl_2/HOAc$	100	<5	40
19 ^{f,i}	CuO	$Cl_2CHCHCl_2/HOAc$	100	<5	45

^a Reaction conditions: 1a (0.6 mmol), 2a (0.4 mmol), catalyst (12 mg), solvent (1.2 mL), air, 20 h. ^b Isolated yields. ^c 12 mg of Cu/OMS-2 (Cu: 1.65 wt%) was used. ^d 12 mg of $Cu(OH)_x/OMS-2$ (Cu: 1.45 wt%) was used. ^e For 3 h. ^f 0.1 mL of HOAc was used to comprise the mixed solvent. ^g Under O_2 . ^h 1 mol% of CuO and 12 mg of H-OMS-2 were used. ⁱ 0.4 mmol of CuO was used.

was also unfruitful, and **3a** was produced in 10% yield with 18% yield of **3aa** (Table 1, entry 4). To our delight, increasing the reaction temperature to 100 °C enhanced the yield of **3a** to 23% with a trace amount of **3aa** when Cu/H-OMS-2 was used as a catalyst (Table 1, entry 5). Next, a lot of solvents were examined to further better the yield of **3a** at 100 °C with Cu/H-OMS-2 (Table 1, entries 6–10). It was found that apolar $\text{Cl}_2\text{CHCHCl}_2$ gave the highest yield of **3a** (41%) in the absence of by-products and HOAc provided 0% yield of **3a** but 59% yield of **3aa** within 3 h in the presence of Cu/H-OMS-2 (Table 1, entries 9 and 10). Therefore, we envisioned that the mixed solvent of HOAc and $\text{Cl}_2\text{CHCHCl}_2$ probably could efficiently transform **3aa** and give **3a** in high yield because HOAc is suited for the generation of Michael adduct **3aa** and able to enhance the electrophilic ability of copper while $\text{Cl}_2\text{CHCHCl}_2$ is superior for the oxidative cyclization. As expected, when we added 0.1 mL of HOAc into 1.2 mL of $\text{Cl}_2\text{CHCHCl}_2$ as a mixed solvent in the reaction, the desired product **3a** was obtained in 89% yield without **3aa** and other by-products (Table 1, entry 11). Subsequently, a series of mixed solvents containing HOAc were investigated, but the results were not satisfying (Table 1, entries 12–14). Also, we found that the oxygen atmosphere did not better the yield of the reaction (Table 1, entry 15). Next, the reaction temperature was changed and the results demonstrated that the reaction did not proceed below 80 °C and higher temperature did not improve the reaction (Table 1, entries 16 and 17). Finally, control experiments of the catalysts were run in the mixed solvent in air at 100 °C. The physical mixture of bulk CuO and H-OMS-2 only gave Michael adduct **3aa** as the main product, while **3a** was barely observed by the use of a stoichiometric amount of bulk CuO in the reaction (Table 1, entries 18 and 19). These observations suggest that the highly dispersed copper species on H-OMS-2 play a key role in the oxidative cyclization and there is an interaction between supported copper and H-OMS-2. As a result of the optimization, we concluded that the best reaction conditions for cyclization of 2-aminopyridine and chalcone in a mixed solvent of $\text{Cl}_2\text{CHCHCl}_2$ /HOAc involve the use of Cu/H-OMS-2 as the catalyst at 100 °C for 20 h with air as the oxidant.

With the optimized conditions in hand, we investigated the substrate scope of the cyclization (Table 2). Firstly, various substituted chalcones were tolerable in the reactions and gave the corresponding 3-arylimidazo[1,2-*a*]pyridines in moderate to good yields (Table 2, **3a**–**3j**). The Michael adduct by-products were not observed in all cases. Generally, chalcones with electron-withdrawing substitutes offered higher yields of desired products than electron-rich chalcones did. Sterically hindered chalcone, like 2-chlorochalcone, did not proceed in the reaction (Table 2, **3e**). On the other hand, a number of substituted 2-aminopyridines smoothly participated in the reactions and provided desired products in good yields without the observation of Michael adducts. Specifically, 2-aminopyridines with electron-donating groups showed higher activity in comparison with the ones with electron-withdrawing groups, such as halogens (Table 2, **3k**–**3w**). More

Table 2 Synthesis of 3-arylimidazo[1,2-*a*]pyridines catalyzed by Cu/H-OMS-2^a



Product	R ¹	R ²	R ³	Yield ^b (%)
3b	H	4-Cl	H	76
3c	H	4-Cl	4-Cl	82
3d	H	H	4-Cl	88
3e	H	2-Cl	H	<5
3f	H	4-OMe	H	79
3g	H	H	4-OMe	65
3h	H	H	3,4-diOMe	45
3i	H	4-NO ₂	H	84
3j	H	4-F	4-Me	60
3k	3-Me	H	H	72
3l	3-Me	4-Cl	4-Cl	71
3m	4-Me	2-Cl	H	<5
3n	4-Me	4-Cl	4-Cl	70
3o	5-Me	H	H	66
3p	5-Me	4-Cl	4-Cl	64
3q	5-Me	H	4-Cl	69
3r	5-Me	4-F	4-Me	53
3s	4-CF ₃	4-Cl	4-Cl	39
3t	3-Br	4-Cl	4-Cl	45
3u	5-Br	4-Cl	4-Cl	42
3v	4-Cl	4-Cl	4-Cl	55
3w	5-Cl	4-Cl	4-Cl	52
—	5-COOMe	H	H	0
—	3-CN	H	H	0

^a Reaction conditions: **1** (0.6 mmol), **2** (0.4 mmol), Cu/H-OMS-2 (12 mg, 0.7 mol%), $\text{Cl}_2\text{CHCHCl}_2$ (1.2 mL), HOAc (0.1 mL), 100 °C, 20 h, air. ^b Isolated yields.

importantly, many multi-halogen-substituted 3-arylimidazo[1,2-*a*]pyridines were obtained in 42–64% yields, which provides opportunities to further functionalize these halogen-substituted products using coupling techniques.¹⁸ Nevertheless, 2-aminopyridines with sensitive groups, like –COOMe and –CN, failed to proceed under the present system because the HOAc of the solvent decomposed these substrates quickly.

In order to further study the generality of this heterogeneous process, 2-aminopyrimidine **5** was used as a substrate to synthesize 3-arylimidazo[1,2-*a*]pyrimidines. Gratifyingly, 2-aminopyrimidine worked very well with chalcones and good yields of 3-arylimidazo[1,2-*a*]pyrimidines **4a**–**4d** were obtained fruitfully (Table 3). To the best of our knowledge, this is the first example that a heterogeneous copper-based material catalyzed the synthesis of 3-arylimidazo[1,2-*a*]pyrimidines between 2-aminopyrimidine and chalcones *via* oxidative C–N bond forming.^{13d} However, steric hindrance affected the reactions significantly (Table 3, **4e**) and the electron-rich substrate, dimethoxychalcone, did not participate in the reaction at all. Unfortunately, 2-aminopyrazine and 2-aminothiazole were not tolerant under the present catalytic system.

From a synthetic point of view, to make this heterogeneous approach to 3-arylimidazo[1,2-*a*]pyridines more

Table 3 Synthesis of 3-arylimidazo[1,2-*a*]pyrimidines catalyzed by Cu/H-OMS-2^a

<p>4a, 76%</p>	<p>4b, 82%</p>	<p>4c, 81%</p>
<p>4d, 46%</p>	<p>4e, 25%</p>	<p>N.R.</p>

^a Reaction conditions: 5 (0.6 mmol), 2 (0.4 mmol), Cu/H-OMS-2 (12 mg, 0.7 mol%), Cl₂CHCHCl₂ (1.2 mL), HOAc (0.1 mL), 100 °C, 20 h, air, isolated yields.

attractive, we investigated their formation *via* a one-pot, three-component reaction sequence that avoids the isolation of the chalcone intermediate. In Cl₂CHCHCl₂, acetophenone reacted with aldehyde catalyzed by Cu/H-OMS-2 in the presence of 2-aminopyridine for 2 h at 100 °C. Then, HOAc was added into the mixture and the reaction was run for 20 h again in air. In this way, this one-pot synthesis gave the corresponding 3-arylimidazo[1,2-*a*]pyrimidines in 52–75% yields without using any additives (Scheme 3).

Finally, recovery and recyclability of the heterogeneous catalyst were studied by the reaction between 2-aminopyridine and 4,4'-dichlorochalcone using 0.7 mol% of Cu/H-OMS-2 in the mixed solvent at 100 °C for 20 h in air. After each run, Cu/H-OMS-2 was easily isolated by centrifugation, then washed by water and finally dried at 110 °C for the next experiment. The image of TEM demonstrated that the morphology of the used Cu/H-OMS-2 is not changed and it is stable on the structure (see the ESI,† Fig. S4). The experimental results showed that Cu/H-OMS-2 could be reutilized four times with an increasing decrease in the catalytic activity and the activity of the catalyst significantly dropped to 48% after four runs (Table 4). After the first run, inductively coupled plasma-atomic emission spectroscopy (ICP-AES) was conducted to analyze the reaction solution after filtration of

Table 4 The recyclability of Cu/H-OMS-2^a

Run	1	2	3	4	5
Isolated yield (%)	82	78	70	65	48

^a Reaction conditions: 2-aminopyridine (0.6 mmol), chalcone (0.4 mmol), Cu/H-OMS-2 (12 mg, 0.7 mol%), Cl₂CHCHCl₂ (1.2 mL), HOAc (0.1 mL), 100 °C, 20 h, air.

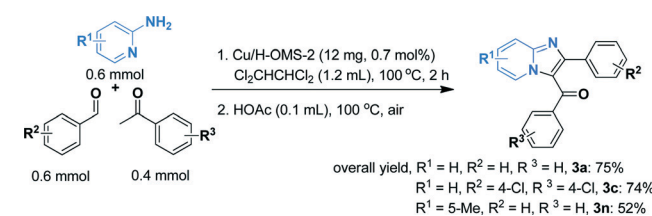
the catalyst, which showed 0.5 ppm of copper leached from Cu/H-OMS-2. The leached copper from the catalyst perhaps incurs the loss of the catalytic activity. Furthermore, a hot filtration experiment (for experiment detail, see the ESI,† Scheme S1) showed that the leached copper species in the solution is catalytically inactive and cannot trigger the reaction at all. Therefore, it is believed that the observed catalysis is derived from the solid catalyst rather than the leached copper species, and the catalyst is heterogeneous in nature.

Conclusions

In conclusion, we have employed Cu/H-OMS-2 as an efficient catalyst in the heterogeneous biomimetic oxidative synthesis of 3-arylimidazo[1,2-*a*]pyrimidines and 3-arylimidazo[1,2-*a*]pyrimidines. The reactions proceed in a mixed solvent of Cl₂CHCHCl₂ and HOAc in the presence of a very low amount of catalyst (Cu: 0.7 mol%) and air as the oxidant without the use of bases and ligands. Moreover, the catalyst can also be applied in one-pot reactions of ketones, aldehydes and 2-aminopyridines. More importantly, the results from H₂-TPR prove that the redox ability of Cu/H-OMS-2 is significantly improved because of the electronic interaction between Cu and H-OMS-2. For the catalyst, the low loading Cu is used as a catalytic metal and H-OMS-2 is used as an ETM as well as an excellent support, which sequentially decreases the redox energy barrier during the oxidative transformation to make the electrons transfer rapidly. Finally, the highly dispersed Cu/H-OMS-2 is naturally heterogeneous and recyclable.

Experimental section

Unless otherwise noted, all reagents were purchased from commercial suppliers and used without further purification. Metal salts were commercially available and were used directly. All experiments were carried out under air conditions. Flash chromatography was carried out with Merck silica gel 60 (200–300 mesh). Analytical TLC was performed with Merck silica gel 60 F254 plates, and the products were visualized by UV detection. ¹H NMR and ¹³C NMR (400 and 100 MHz, respectively) spectra were recorded in CDCl₃. Chemical shifts (δ) are reported in parts per million using TMS as the internal standard, and spin–spin coupling

**Scheme 3** One-pot synthesis of 3-arylimidazo[1,2-*a*]pyrimidines from ketone, aldehyde and 2-aminopyridine.

constants (J) are given in hertz. Cu/OMS-2 (ref. 9a) (2.0 wt% theoretical loading, actual loading is 1.65 wt%) was synthesized by wet impregnation in deionized water, and Cu(OH)_x/OMS-2 (ref. 9b) (2.0 wt% theoretical loading, actual loading is 1.45 wt%) was made by deposition-precipitation in water.

Catalyst characterization methods

The crystal phase and composition of catalysts were determined by powder X-ray diffraction using an X-Pert PRO X-ray diffractometer with CuK α radiation in the 2θ range of 10–90°. Infrared spectra of the materials were recorded with calcined powders dispersed in KBr (2 mg of the sample in 300 mg of KBr) using a Perkin-Elmer One FTIR spectrometer with a resolution of 4 cm⁻¹ operating in the range 500–2000 cm⁻¹ with 4 scans per spectrum. The morphologies of the samples were characterized by using a TF20 transmission electron microscope and SM-5600LV scanning electron microscope. Nitrogen adsorption-desorption measurements were performed at 76 K using an ASAP 2020M analyzer utilizing the BET model for the calculation of specific surface areas. The reducibility of the catalysts was measured by the hydrogen temperature-programmed reduction (H₂-TPR) technique. 50 mg of OMS-2, H-OMS-2 or Cu/H-OMS-2 was placed in a quartz reactor that was connected to a TPR apparatus, and the reactor was heated from r.t. to 550 °C with a heating rate of 10 °C min⁻¹. The reducing atmosphere was a mixture of H₂ and N₂ with a total flow rate of 30 mL min⁻¹ and the amount of H₂ uptake during the reduction was measured by using a thermal conductivity detector (TCD). The oxygen species of the catalysts was investigated by the oxygen temperature-programmed desorption (O₂-TPD) technique. 50 mg of H-OMS-2 or Cu/H-OMS-2 was placed in a quartz reactor that was connected to a TPD apparatus and the reactor was purged with He at room temperature for 1 h followed by heating to 950 °C at a heating rate of 10 °C min⁻¹ in the same atmosphere.

Preparation of H-OMS-2 (ref. 4c)

H-OMS-2 was synthesized by ion exchange with homemade OMS-2. The concentrated HNO₃ (50 mL) was added to OMS-2 (2 g) and the slurry was stirred vigorously at 80 °C for 6 h. The product was filtered and washed by deionized water many times. Then, the product was dried at 120 °C for 12 h in an oven and calcined at 280 °C for 6 h.

Preparation of Cu/H-OMS-2

Support H-OMS-2 (2 g) was added to a 50 mL round-bottom flask. A solution of Cu(NO₃)₂·3H₂O (0.15 g) in deionized water (10 mL) was added to H-OMS-2, and additional deionized water (10 mL) was added to wash down the sides of the flask. Then the flask was submerged into an ultrasound bath for 3 h at room temperature and stirred for further 20 h at room temperature. After that, the water was distilled under reduced pressure on a rotary evaporator at 80 °C for more than 2 h. Finally, the black powder was dried in an oven at 110 °C for

4 h followed by calcination at 350 °C in air for 2 h. The black powder Cu/OMS-2 (2.0 wt% theoretical loading, the actual loading is 1.58 wt%) was characterized by ICP-OES, BET, XRD, XPS, FTIR, TEM, SEM, H₂-TPR and O₂-TPD techniques.

General procedure for Cu/H-OMS-2-catalyzed 3-arylimidazo-[1,2-*a*]pyridines synthesis

Cu/H-OMS-2 (12 mg, 0.7 mol%), 2-aminopyridine (0.6 mmol), chalcones (0.4 mmol) and Cl₂CHCHCl₂ (1.2 mL)/HOAc (0.1 mL) were added to a flask with a bar. The flask was stirred at 100 °C for 20 h in air. After cooling to room temperature, the mixture was diluted with ethyl acetate and filtered. The filtrate was removed under reduced pressure to get the crude product, which was further purified by silica gel chromatography (petroleum/ethyl acetate = 4/1 as the eluent) to yield the corresponding product. The identity and purity of the products were confirmed by ¹H and ¹³C NMR spectroscopic analyses.

Acknowledgements

We gratefully acknowledge the National Natural Science Foundation of China (Grant No. 21403256, 21573261, and 21372102) and the Suzhou Industrial Technology and Innovation Project (Grant No. SYG201531).

Notes and references

- (a) S. L. Suib, *Acc. Chem. Res.*, 2008, **41**, 479–487; (b) S. L. Suib, *J. Mater. Chem.*, 2008, **18**, 1623–1631; (c) Y. F. Shen, R. P. Zerger, R. N. DeGuzman, S. L. Suib, L. McCurdy, D. I. Potter and C. L. O'Young, *Science*, 1993, **260**, 511–515.
- (a) R. N. DeGuzman, Y.-F. Shen, E. J. Neth, S. L. Suib, C.-L. O'Young, S. Levine and J. M. Newsam, *Chem. Mater.*, 1994, **1**, 815–821; (b) Y. C. Son, V. D. Makwana, A. R. Howell and S. L. Suib, *Angew. Chem., Int. Ed.*, 2001, **40**, 4280–4283; (c) R. Ghosh, X. Shen, J. C. Villegas, Y. Ding, K. Malinger and S. L. Suib, *J. Phys. Chem. B*, 2006, **110**, 7592–7599.
- (a) K. Yamaguchi, Y. Wang and N. Mizuno, *ChemCatChem*, 2013, **5**, 2835–2838; (b) K. Yamaguchi, H. Kobayashi, Y. Wang, T. Oishi, Y. Ogasawara and N. Mizuno, *Catal. Sci. Technol.*, 2013, **3**, 318–327; (c) Y. Wang, H. Kobayashi, K. Yamaguchi and N. Mizuno, *Chem. Commun.*, 2012, **48**, 2642–2644; (d) K. Yamaguchi, H. Kobayashi, T. Oishi and N. Mizuno, *Angew. Chem., Int. Ed.*, 2012, **51**, 544–547; (e) X. Meng, J. Zhang, G. Chen, B. Chen and P. Zhao, *Catal. Commun.*, 2015, **69**, 239–242; (f) X. Jin, K. Yamaguchi and N. Mizuno, *RSC Adv.*, 2014, **4**, 34712–34715.
- For the selected papers on the application of modified OMS-2 in oxidations, see: (a) R. Kumar, S. Sithambaram and S. L. Suib, *J. Catal.*, 2009, **262**, 304–313; (b) X. Chen, Y. Shen, S. L. Suib and C. L. O'Young, *Chem. Mater.*, 2002, **14**, 940–948; (c) V. P. Santos, O. S. G. P. Soares, J. J. W. Bakker, M. F. R. Pereira, J. J. M. Órfão, J. Gascon, F. Kapteijn and J. L. Figueiredo, *J. Catal.*, 2012, **293**, 165–174; (d) S. Sithambaram, R. Kumar, Y.-C. Son and S. L. Suib, *J. Catal.*, 2008, **253**,

- 269–277; (e) Y.-G. Yin, W.-Q. Xu and S. L. Suib, *Inorg. Chem.*, 1995, **34**, 4187–4193.
- 5 (a) X.-S. Liu, Z.-N. Jin, J.-Q. Lu, X.-X. Wang and M.-F. Luo, *Chem. Eng. J.*, 2010, **162**, 151–157; (b) W. Y. Hernández, M. A. Centeno, S. Ivanova, P. Eloy, E. M. Gaigneaux and J. A. Odriozola, *Appl. Catal., B*, 2012, **123**, 27–35; (c) M. Özacara, A. S. Poyraz, H. C. Genuino, C.-H. Kuo, Y. Meng and S. L. Suib, *Appl. Catal., A*, 2013, **462**, 64–74.
- 6 M. Sun, L. Yu, F. Ye, G. Diao, Q. Yu, Z. Hao, Y. Zheng and L. Yuan, *Chem. Eng. J.*, 2013, **220**, 320–327.
- 7 Y. Yang, J. Huang, S. Zhang, S. Wang, S. Deng, B. Wang and G. Yu, *Appl. Catal., B*, 2014, **150**, 167–178.
- 8 For the selected papers on the application of ETMs in homogeneous catalysis, see: (a) J. Piera and J. E. Bäckvall, *Angew. Chem., Int. Ed.*, 2008, **47**, 3506–3523; (b) B. P. Babu, X. Meng and J. E. Bäckvall, *Chem. – Eur. J.*, 2013, **19**, 4140–4145; (c) Y. Endo and J. E. Bäckvall, *Chem. – Eur. J.*, 2012, **18**, 13609–13613; (d) X. Meng, C. Li, B. Han, T. Wang and B. Chen, *Tetrahedron*, 2010, **66**, 4029–4031; (e) N. Gigant and J. E. Bäckvall, *Org. Lett.*, 2014, **16**, 1664–1667; (f) N. Gigant and J. E. Bäckvall, *Org. Lett.*, 2014, **16**, 4432–4435; (g) N. Gigant and J. E. Bäckvall, *Chem. – Eur. J.*, 2013, **19**, 10799–10803.
- 9 (a) X. Meng, C. Yu, G. Chen and P. Zhao, *Catal. Sci. Technol.*, 2015, **5**, 372–379; (b) T. Oishi, K. Yamaguchi and N. Mizuno, *ACS Catal.*, 2011, **1**, 1351–1354.
- 10 (a) J. C. Teulade, G. Grassy, J. P. Girard and J. P. Chapat, *Eur. J. Med. Chem.*, 1978, **13**, 271–276; (b) A. Gueiffier, M. Lhassani, A. Elhakmaoui, R. Snoeck, G. Andrei, O. Chaxignon, J. C. Teulade, A. Kerbal, E. M. Essassi, J. C. Debouzy, M. Witvrouw, Y. Blache, J. Balzarini, E. De Clercq and J. P. Chapat, *J. Med. Chem.*, 1996, **39**, 2856–2859; (c) M. Hranjec, I. Piantanida, M. Kralj, L. Suman, K. Pavelić and G. Karminski-Zamola, *J. Med. Chem.*, 2008, **51**, 4899–4910; (d) C. Hamdouchi, J. De Blas, M. del Prado, J. Gruber, B. A. Heinz and L. Vance, *J. Med. Chem.*, 1999, **42**, 50–59.
- 11 M. Baumann, I. R. Baxendale, S. V. Ley and N. Nikbin, *Beilstein J. Org. Chem.*, 2011, **7**, 442–495.
- 12 (a) Y.-S. Tung, M. S. Coumar, Y.-S. Wu, H.-Y. Shiao, J.-Y. Chang, J.-P. Liou, P. Shukla, C.-W. Chang, C.-Y. Chang, C.-C. Kuo, T.-K. Yeh, C.-Y. Lin, J.-S. Wu, S.-Y. Wu, C.-C. Liao and H.-P. Hsieh, *J. Med. Chem.*, 2011, **54**, 3076–3080; (b) H.-P. Hsieh, Y.-S. Chao, J.-P. Liou, J.-Y. Chang and Y.-S. Tung, Antitumor compounds. US7456289, 2008.
- 13 (a) K. Monir, A. K. Bagdi, S. Mishra, A. Majee and A. Hajra, *Adv. Synth. Catal.*, 2014, **356**, 1105–1112; (b) P. Kaswan, K. Pericherla, H. K. Saini and A. Kumar, *RSC Adv.*, 2015, **5**, 3670–3677; (c) P. Kaswan, K. Pericherla, Rajnikant and A. Kumar, *Tetrahedron*, 2014, **70**, 8539–8544; (d) K. R. Reddy, A. S. Reddy, R. Shankar, R. Kant and P. Das, *Asian J. Org. Chem.*, 2015, **4**, 537–583.
- 14 S. Goswami, S. Jana, A. Hazra and A. K. J. Adak, *J. Heterocycl. Chem.*, 2007, **44**, 1191–1194.
- 15 For selected examples of heterogeneous catalytic organic synthesis, see: (a) K. Natte, H. Neumann and X.-F. Wu, *Catal. Sci. Technol.*, 2015, **5**, 4474–4480; (b) X. Meng, X. Xu, T. Gao and B. Chen, *Eur. J. Org. Chem.*, 2010, 5409–5414; (c) A. T. Nguyen, L. T. Pham, N. T. S. Phan and T. Truong, *Catal. Sci. Technol.*, 2014, **4**, 4281–4288; (d) X. Meng, Y. Wang, C. Yu and P. Zhao, *RSC Adv.*, 2014, **4**, 27301–27307; (e) X. Meng, C. Yu and P. Zhao, *RSC Adv.*, 2014, **4**, 8612–8616; (f) J. Chen, L. He, K. Natte, H. Neumann, M. Beller and X.-F. Wu, *Adv. Synth. Catal.*, 2014, **356**, 2955–2959.
- 16 M. Ousmane, G. Perrussel, Z. Yan, J.-M. Clacens, F. De Campo and M. Pera-Titus, *J. Catal.*, 2014, **309**, 439–452.
- 17 V. P. Santos, M. F. R. Pereira, J. J. M. Órfão and J. L. Figueiredo, *Appl. Catal., B*, 2010, **99**, 353–363.
- 18 (a) S. V. Ley and A. W. Thomas, *Angew. Chem., Int. Ed.*, 2003, **42**, 5400–5449; (b) C. C. C. J. Seechurn, M. O. Kitching, T. J. Colacot and V. Snieckus, *Angew. Chem., Int. Ed.*, 2012, **51**, 5062–5085.